Ultrastable nanostructured polymer glasses

Yunlong Guo[1], Anatoli Morozov[2], Dirk Schneider[3], Jae Woo Chung[1], Chuan Zhang[1],
Maike Waldmann[4], Nan Yao[4], George Fytas[3,5], Craig B. Arnold[2,4] and Rodney D. Priestley[1,4]★

Owing to the kinetic nature of the glass transition, the ability to significantly alter the properties of amorphous solids by the typical routes to the vitreous state is restricted. For instance, an order of magnitude change in the cooling rate merely modifies the value of the glass transition temperature (T_g) by a few degrees. Here we show that matrix-assisted pulsed laser evaporation (MAPLE) can be used to form ultrastable and nanostructured glassy polymer films which, relative to the standard poly(methyl methacrylate) glass formed on cooling at standard rates, are 40% less dense, have a 40 K higher T_g, and exhibit a two orders of magnitude enhancement in kinetic stability at high temperatures. The unique set of properties of MAPLE-deposited glasses may make them attractive in technologies where weight and stability are central design issues.

Conceptually, glasses are liquids that have lost their ability to flow[1]. They are typically formed by cooling from the liquid state[2,3]. If the liquid is cooled at sufficiently high rates, crystallization can be circumvented beyond the melting temperature. Eventually, on further cooling, molecular motions become progressively slower, and the molecules are unable to adequately sample equilibrium configurations in the experimental timescale, as set by the rate of cooling. The temperature at which the liquid falls out of equilibrium is denoted as the glass transition temperature (T_g). The glass transition is a kinetic phenomenon[4]. The slower the rate of cooling during glass formation, the greater is the available time for molecular rearrangement in the liquid state. Consequently, the liquid will be cooled to a lower temperature before it abruptly transforms into a glass. The properties of glasses, hence, depend on the path to the glassy state, and may be tuned by the rate of cooling. From a practical viewpoint, an order of magnitude change in the rate of cooling merely modifies the value of T_g by ~3 K (ref. 5). Thus, the ability to tune the properties of glasses through the typical route to the vitreous state is restricted, and therefore other routes to the glassy state—those that can bypass the kinetic limitations of glass formation—are necessary to induce significant changes in material properties.

In a noteworthy discovery, Ediger and co-workers showed that organic molecular glasses with exceptional thermodynamic and kinetic stability (that is, 'stable' glasses) could be formed by physical vapour deposition (PVD; ref. 6). By carefully controlling deposition rate and substrate temperature, vapour-deposited molecular glasses exhibited an ~8 J g^{-1} decrease in enthalpy, an ~2% increase in density and an ~20% enhancement in elastic modulus[6,7]. By the method of supercooling, it has been estimated that gradual cooling over ~1,000 yr would be required to obtain similar properties to those of the vapour-deposited glasses[8,9]. Furthermore, the vapour-deposited glasses are kinetically stable, requiring approximately three orders of magnitude greater time to complete the glass to liquid transition when annealed at T_g (ref. 10). Although the initial discovery of stable glasses was for indomethacin and trisnapthylbenzene, toluene[11] and ethylbenzene[12] stable glasses have also been produced.

The formation of the analogous stable polymer glasses represents a major technological and scientific challenge because of the inability to deposit polymers using PVD and the inherently slower chain conformations owing to the increased molecular weight. Here, we sought the development of the first stable polymer glasses using a unique deposition method termed matrix-assisted pulsed laser evaporation (MAPLE). We have discovered that MAPLE can be used to form glassy polymer films with enhanced values of T_g and superior kinetic stability. Relative to the standard glass formed on cooling at standard rates, glasses prepared using MAPLE can have ~30–40 K higher values of T_g. Furthermore, the kinetic stability in the glassy state can be enhanced by two orders of magnitude. However, contrary to stable organic molecular glasses, which show an increase in density, our stable polymer glasses exhibit an ~40% reduction in density. Despite the change in density of stable polymer glasses, their modulus remains unchanged from the standard glass. The unique combination of properties is a result of the glass morphology created during MAPLE deposition. We have developed glassy films formed by the assembly of nearly spherical polymer nanoglobules, that is, a supramolecular nanostructured glass, the properties of which we suggest are dictated by those of the individual nanoglobules and their collective packing.

In the MAPLE method, a pulsed laser ablates a target, consisting of a frozen dilute solution of the desired polymer, to produce films of the material[13,14]. As opposed to direct polymer ablation, MAPLE provides a gentle and non-destructive means for the deposition of polymer films[14]. Figure 1a compares the heat capacity curves of standard, hyperquenched, and MAPLE-deposited poly(methyl methacrylate) (PMMA). Formation of the standard glass was achieved by cooling from the liquid at 40 K min^{-1} to 293 K. Formation of the hyperquenched glass was achieved by rapidly transferring molten PMMA contained in an aluminium pan into liquid nitrogen, the estimated cooling rate of the process being ~120 K s^{-1} (ref. 15). The MAPLE-deposited glass was formed by the slow deposition of PMMA (growth rate ~0.25 nm s^{-1}) onto a silica substrate held at a substrate temperature ($T_{substrate}$) of 311 K (Supplementary Information). The black curve in Fig. 1a represents the heat capacity of the standard PMMA glass, and $T_{g,standard}$ = 359 K is the midpoint standard

[1]Department of Chemical and Biological Engineering, Princeton University, Princeton, New Jersey 08544, USA, [2]Department of Mechanical and Aerospace Engineering, Princeton University, Princeton, New Jersey 08544, USA, [3]Max Planck Institut für Polymerforschung, Ackermannweg 10, 55128 Mainz, Germany, [4]Princeton Institute for the Science and Technology of Materials, Princeton University, Princeton, New Jersey 08544, USA, [5]Department of Materials Science, University of Crete and FORTH., P.O. Box 1527, 71110, Heraklion, Greece. *e-mail: rpriestl@princeton.edu.

glass transition temperature, as determined from the peak of the derivative of the heat capacity curve (see Fig. 1b and Supplementary Information). The red and green curves represent the heat capacities of the hyperquenched and MAPLE-deposited PMMA, respectively. Whereas the hyperquenched glass exhibits signatures of the well-known enthalpy recovery exotherm below $T_{g,standard}$ and a modest T_g enhancement of ~5 K (ref. 16), the heat capacity curve is noticeably different for the MAPLE-deposited PMMA. For instance, the glassy-state heat capacity is significantly lower for the latter. Remarkably, an enhancement in T_g of ~33 K is observed for the MAPLE-deposited glass (midpoint $T_{g,MAPLE} = 392$ K; Fig. 1b).

To locate the relative position of the standard, hyperquenched and MAPLE-deposited glasses on the energy landscape[17], we computed the enthalpy of the materials by taking the integral of the heat capacity. Figure 1c compares the enthalpy curves of the PMMA samples. MAPLE-deposited PMMA exhibited a greater enthalpy. For instance, at 340 K, the enthalpy difference between the MAPLE-deposited glass and standard glass was ~30 J g^{-1}.

The major improvement in thermal stability, as evident by calorimetry, was supported by temperature-dependent wide-angle X-ray scattering (WAXS) and Brillouin light scattering (BLS) studies. As shown in Fig. 2a and b, an abrupt leftwards shift in the scattering curve near the peak at $2\theta \sim 12.7°$, an indication of the glass-to-liquid transformation, occurred at an ~28 K higher temperature for the MAPLE-deposited glass than for the standard glass. Figure 2c plots the variation of the longitudinal sound velocity as a function of temperature for standard and MAPLE-deposited glasses. The characteristic kink in the curve, corresponding to the glass transition[18], distinctly occurred at a higher temperature for the latter. Furthermore, an abrupt increase of the BLS intensity (see lower inset in Fig. 2c) occurred near the onset $T_{g,MAPLE} = 380$ K.

The enhancement in thermal stability of MAPLE-deposited glassy films is accompanied by a significant reduction in density. From refractive index measurements at room temperature, the densities of MAPLE-deposited and standard PMMA were determined to be 0.681 ± 0.008 g cm^{-3} and 1.184 ± 0.002 g cm^{-3}, respectively (Supplementary Information). Hence, MAPLE-deposited PMMA films have an ~42% reduction in density, as estimated from refractive-index measurements. From the X-ray reflectivity (XRR), the reduction in density was estimated to be ~38% for MAPLE-deposited PMMA (Supplementary Information). Remarkably, quenched MAPLE-deposited (Supplementary Information) and standard PMMA glasses exhibited similar sound velocities at $T < T_{g,standard}$, suggesting a similar glassy-state rigidity, in spite of the significantly reduced density for the former (solid diamonds in Fig. 2c; see Methods for the BLS protocol and Supplementary Information).

We note that MAPLE-deposited glasses can be transformed into the standard glass by high-temperature ($T > T_{g,MAPLE}$) annealing followed by subsequent cooling at 40 K min^{-1}. The blue curve in Fig. 1a represents the immediate heating scan of the resulting glass. The agreement between the heat capacity curves of the two glasses formed on cooling provide substantial evidence that MAPLE does not impart any permanent structural change to the glass, and is in agreement with gel permeation chromatography (GPC), nuclear magnetic resonance (NMR) and Fourier transform infrared spectroscopy (FTIR) investigations presented in the Supplementary Information.

While maintaining a constant growth rate, we have investigated the impact of substrate temperature on the thermal stability of MAPLE-deposited glasses. Figure 3a shows the influence of $T_{substrate}$ on the heat capacity of MAPLE-deposited glasses grown at a rate of ~0.25 nm s^{-1}. The green and blue curves represent the first and second heating scans, respectively, of the MAPLE-deposited glass with $T_{substrate} = 311$ K during deposition. The absence of exotherms on heating indicates structural stability. Glasses deposited outside a critical temperature range of ~308–311 K exhibited pronounced
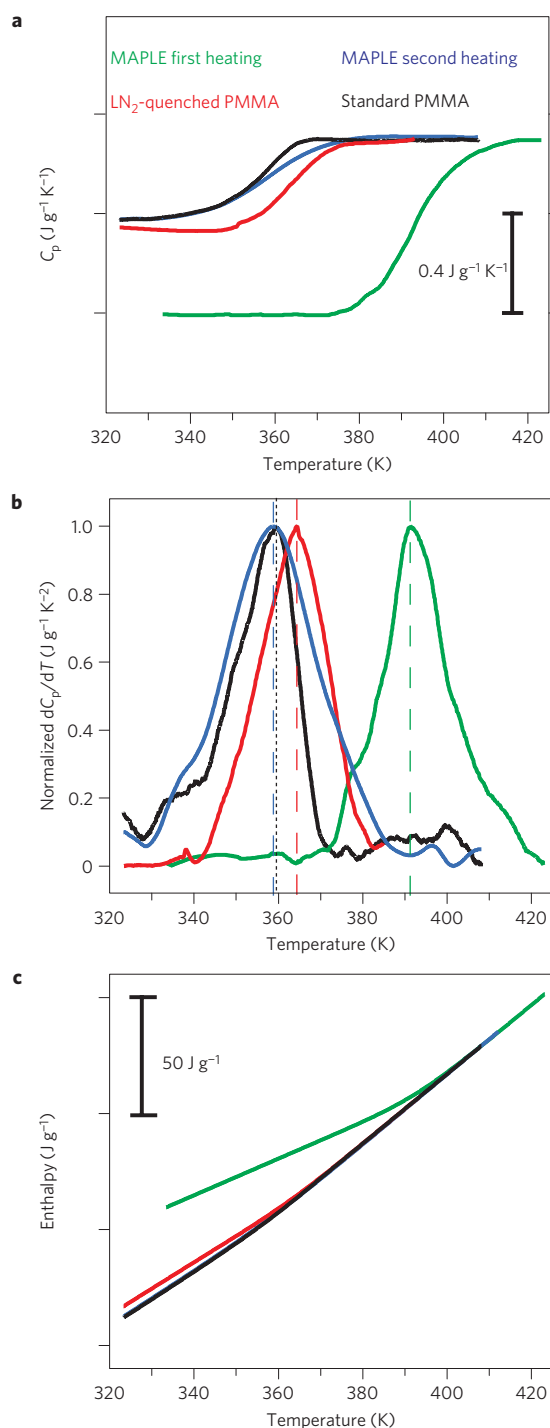
Figure 1 | Effect of processing method on the glass transition temperature of PMMA. a, Heat capacity of PMMA samples: MAPLE-deposited PMMA on first heating (green curve) and second heating (blue curve), hyperquenched PMMA (red curve), and standard PMMA (black curve). All heating rates were 20 K min^{-1}. **b**, Normalized derivatives of heat-capacity curves shown in **a**; the peak of each curve represents the midpoint T_g. **c**, Enthalpy curves of PMMA samples obtained by integration of the heat capacity curves.

exothermic peaks on heating, which would indicate some level of structural instability. However, it is important to note that the onset temperatures of the exothermic peaks were near to the onset of $T_{g,standard}$ whereas the midpoint T_g values of the MAPLE-deposited glasses were ~$T_{g,standard} + 37$–42 K.
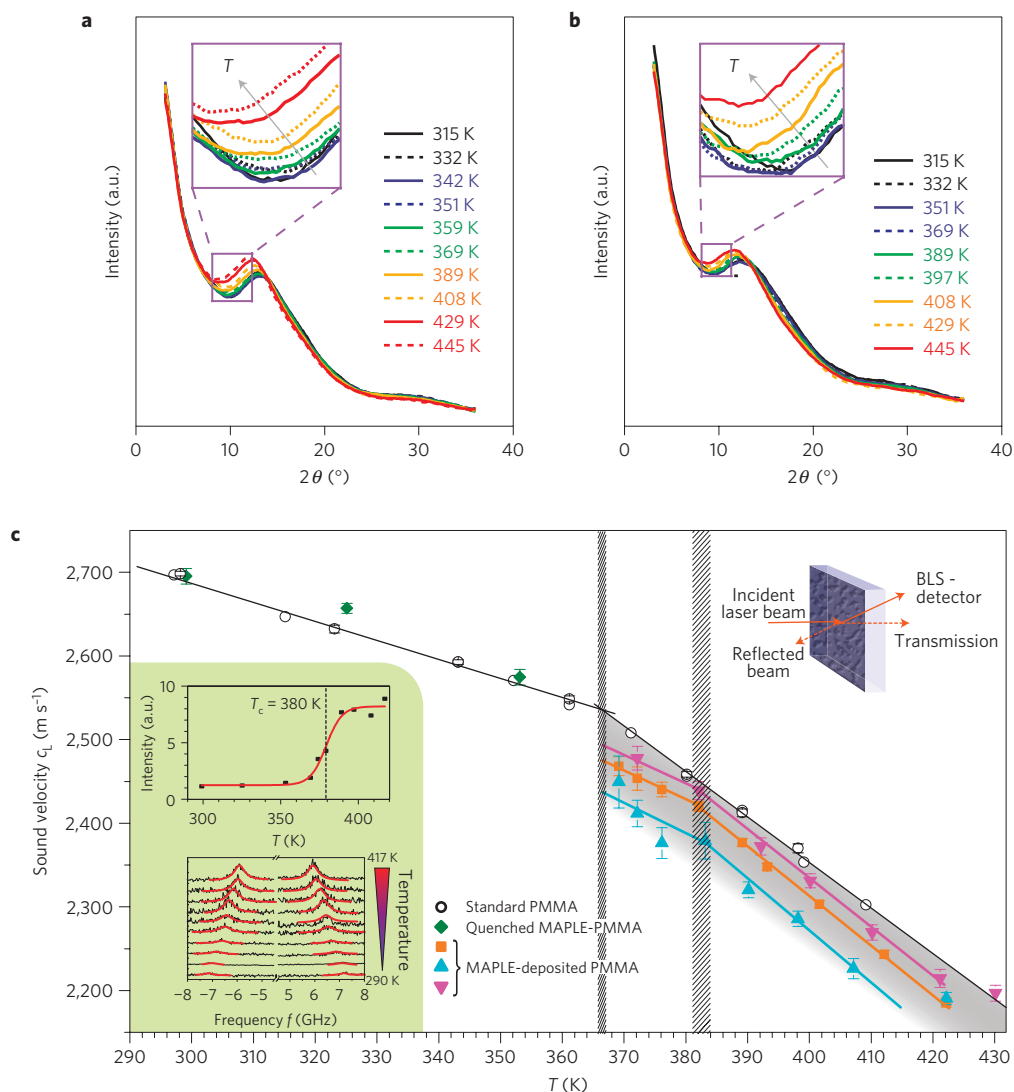
Figure 2 | Structure and elasticity of MAPLE-deposited PMMA films. a,b, Temperature-dependent WAXS patterns of standard (**a**) and MAPLE-deposited PMMA ($T_{substrate} = 311$ K) (**b**). Abrupt leftwards shifts in the curve near the peak, an indication of the glass-to-liquid transformation, occurred at approximately 369 K and 397 K, for standard and MAPLE-deposited PMMA, respectively. **c**, Temperature-dependent longitudinal adiabatic sound velocity obtained from the BLS spectra (spectra shown in lower inset) recorded in a transmission geometry (upper inset). The vertical hatched areas denote the regions of the respective glass transition temperatures of the standard (open circles) and MAPLE-deposited PMMA (solid symbols in the shaded area). The glass–liquid transformation was also estimated from the abrupt increase of the temperature-dependent BLS intensity caused by decreased opaqueness of the film (lower inset) and found to be consistent with DSC measurements. Error bars represent the standard deviation.

Figure 3b plots the enthalpy curves of MAPLE-deposited glasses for different values of $T_{substrate}$ during deposition. All curves were obtained on heating from well below T_g. The minimum enthalpy difference between the MAPLE-deposited and standard glasses was obtained at $T_{substrate} = 311$ K whereas the maximum in the difference was obtained at $T_{substrate} = 300$ K. In spite of being trapped in states of high energy, surprisingly, all glasses exhibit improved thermal stability over the standard glass. That is, relaxation of excess enthalpy, if at all, does not occur until temperatures higher than $T_{g,standard}$. The thermal stability of MAPLE-deposited glasses was strongly dependent on substrate temperature. When formed at $T_{substrate} = 308$ K and 311 K, MAPLE-deposited glasses showed no evidence of structural relaxation as they transformed into the liquid.

In this study, the fictive temperature, T_f, a measure of the glass structure, of MAPLE-deposited glasses was determined using data presented in Fig. 3b. For each sample, T_f was determined by extrapolating the linear portion of the glass line to the point at which it intersected with the liquid line of the standard glass.

The point of intersection between the two lines defined the value of T_f. All MAPLE-deposited glasses exhibited values of T_f higher than the standard glass. Figure 3c shows the influence of $T_{substrate}$ on the values of T_f of PMMA glasses prepared using MAPLE. The maximum values of T_f and $T_f/T_{g,standard}$ were 443 K and 1.24, respectively, at $T_{substrate} = 300$ K. In the temperature range investigated, a substrate temperature of $\sim 0.79 T_{g,MAPLE}$ clearly yielded glasses with the lowest T_f.

That MAPLE-deposited glasses exhibit significantly improved stability is made further apparent by kinetic studies of the quasi-isothermal glass-to-liquid transformation at the midpoint glass transition temperature by means of temperature-modulated differential scanning calorimetry (TMDSC). In these studies, glasses were annealed at their corresponding T_g while the heat flow required to maintain the set temperature was obtained; the reversing heat capacity ($C_{p,rev}$) is proportional to the heat flow. Figure 3d plots $C_{p,rev}$ versus annealing time for the standard glass (black curve), the hyperquenched glass (red curve) and the MAPLE-deposited glass
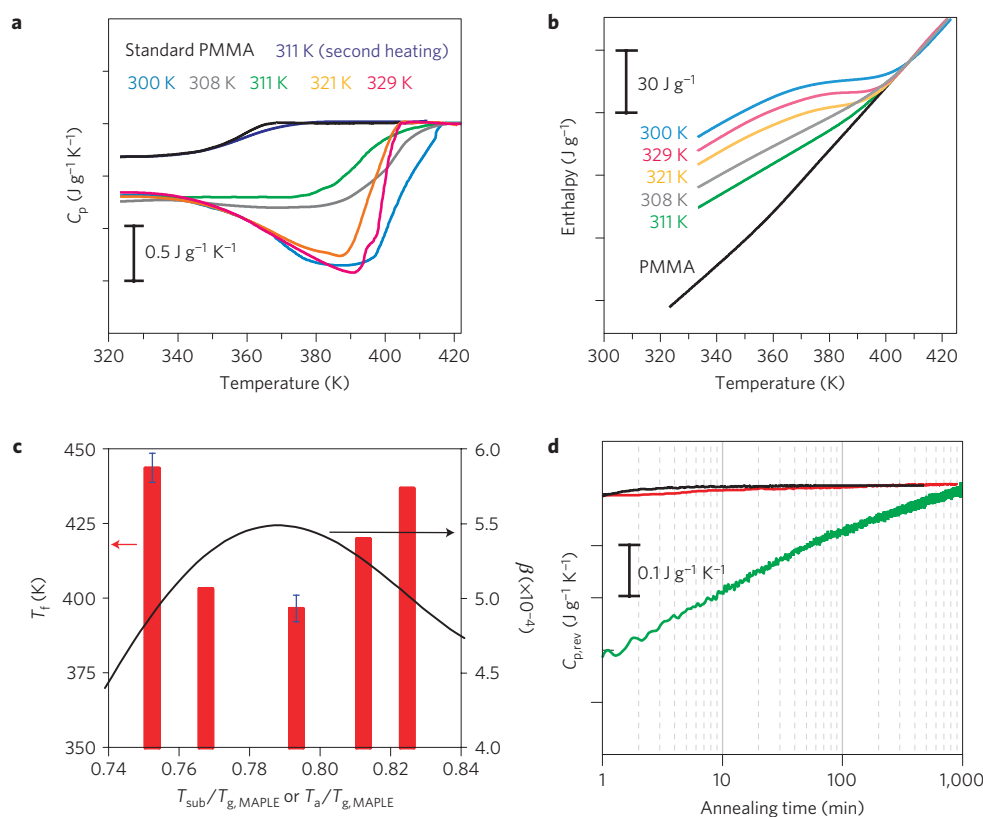
Figure 3 | Dependence of thermal and kinetic stability of MAPLE-deposited PMMA on substrate temperature. a, Heat capacity of standard PMMA and MAPLE-deposited PMMA samples prepared at substrate temperatures ranging from 300 K to 329 K. Lines are colour-coded with the listed substrate temperature. **b**, Enthalpy curves of standard and MAPLE-deposited PMMA samples. **c**, Fictive temperature of PMMA samples prepared using MAPLE plotted as a function of $T_{sub}/T_{g,MAPLE}$. The black curve is the glassy-state structural relaxation rate, β, of PMMA as a function of $T_a/T_{g,MAPLE}$, where T_a is the ageing temperature[18]. Error bars represent the standard deviation. **d**, Reversing heat capacity as a function of time for PMMA samples: standard PMMA (black curve), hyperquenched PMMA (red curve) and MAPLE-deposited PMMA at $T_{substrate} = 311$ K (green curve).

with $T_{substrate} = 311$ K (green curve). As T_g for the samples could not be determined before annealing, estimations were based on the average of three prior measurements. Therefore, $T_{annealing} = 359$ K for the standard glass, 364 K for the hyperquenched glass, and 392 K for the MAPLE-deposited glass. For the standard and hyperquenched glasses, the time required to complete the glass-to-liquid transformation was less than 500 s. For the MAPLE-deposited glass, $\sim 5 \times 10^4$ s was required for the complete transformation, which is two orders of magnitude greater than that necessary for the standard glass. The enhancement in kinetic stability of PMMA glasses prepared using MAPLE is extraordinary, especially when the difference in annealing temperatures of ~ 33 K is considered.

Stable polymeric glasses formed using MAPLE are uniquely different from molecular stable glasses formed using PVD. Although both types of glasses show exceptional thermal and kinetic stability, structurally, they are different. Stable polymeric and molecular glasses exhibit lower and greater densities, respectively, compared with the analogous standard glass. Furthermore, stable molecular glasses can show anisotropy in film structure[19]; whereas stable polymer glasses do not, as evident from BLS measurements performed normal and parallel to the film surface. We suggest that the structural differences are a result of different mechanisms of film formation. In the formation of stable molecular glasses, slow deposition rates coupled with an enhanced surface mobility within the first few nanometres of a film's surface have been postulated as the mechanism of stable glass formation; that is, these two parameters give the molecules extra time to configurationally rearrange towards equilibrium and densify[6]. We note that both experiments[20–22] and simulations[23,24] suggest that glasses possess a layer of enhanced

mobility at the free interface. Furthermore, the dependence of stable glass formation on growth rate and substrate temperature provides significant credibility to the proposed mechanism[8,9], as do recent simulation studies showing that surface molecules are able to sample the energy landscape more effectively than those in the interior[25] and that stable glasses exhibit a distinct layered structure due to reorganization in the enhanced mobile layer[26].

The formation of stable polymer glasses using MAPLE is markedly different. We propose that film formation proceeds by the assembly of nearly spherical polymer nanoglobules[27,28]. Using MAPLE, glasses are formed by the slow deposition of polymer from a frozen target. At low solution concentrations, per laser pulse, tens to thousands of polymer chains may depart the frozen matrix in the same time interval[29]. With the sudden attainment of sufficiently high energy, we propose that clusters of polymer chains collapse into stable globules owing to solvent evaporation during deposition and after landing on the substrate. We note that the recent simulation studies of the MAPLE process reveal the formation of isolated polymer/solvent clusters during transport from the target to the substrate[30]. The improved stability of globules may be due to their formation in vacuum, an environment that should provide a strong thermodynamic force for polymer chain collapse[31,32]. Moreover, there is evidence that glass formation via concentration jumps enhances glass stability[33,34]. Stripping of solvent from polymer/solvent clusters during globule formation could effectively mimic the formation of concentration glasses, thus improving stability. Furthermore, it has been observed that polymer nanoglobules exhibit an enhanced T_g (refs 35,36). The concurrent enhancement/reduction in stability/density, respectively, of
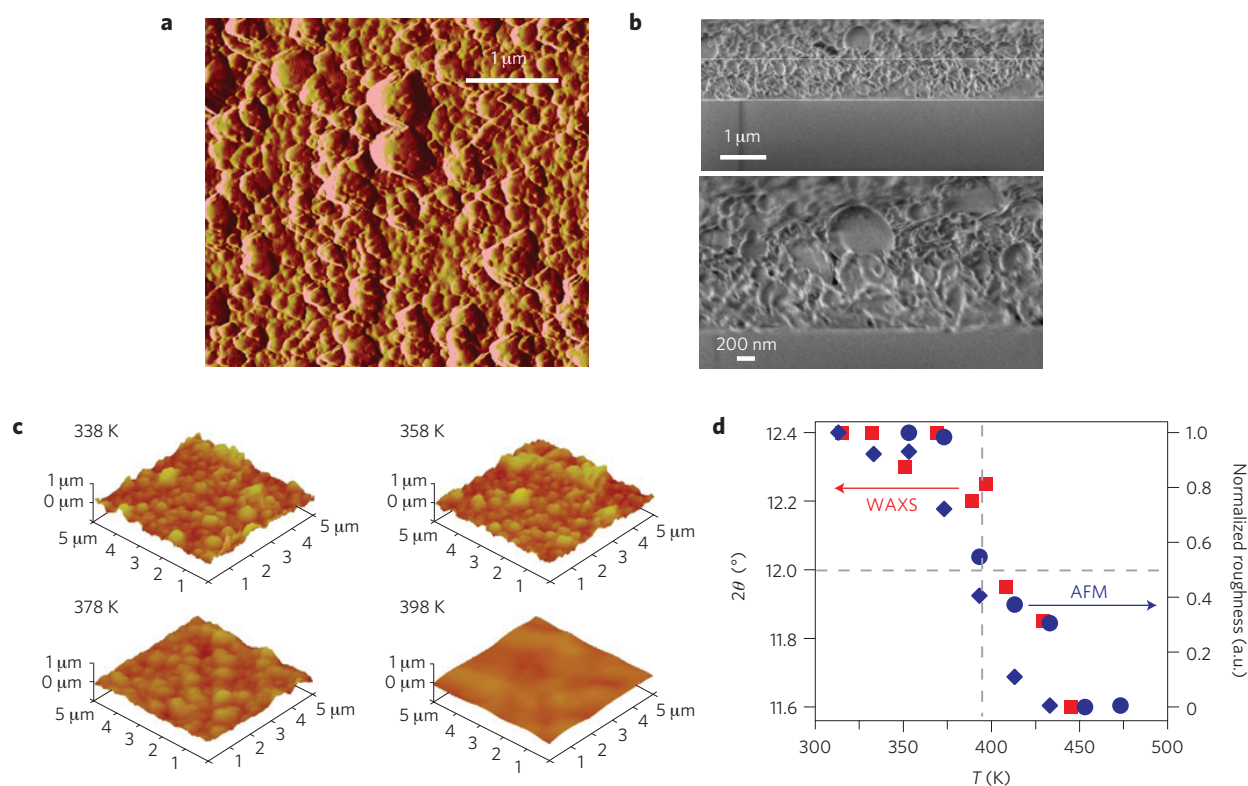
Figure 4 | Morphology of MAPLE-deposited PMMA films. a,b, AFM-amplitude image (**a**) and cross-sectional SEM image (**b**) of MAPLE-deposited PMMA film with $T_{substrate} = 311$ K. **c**, AFM images showing the temperature dependence of the nanostructured topology of MAPLE-deposited films. Although $T_{g,standard} = 359$ K and $T_{g,MAPLE} = 392$ K, remnants of surface nanostructures are present at 398 K. **d**, Temperature dependence of the position of the scattering peak from WAXS scans, and normalized film surface roughness from AFM.

MAPLE-deposited glasses could then be qualitatively explained by the above mechanism of glass formation. That is, whereas individual collapsed globules could promote stability, limiting coalescence of the globules could result in the observed low densities.

Consistent with our proposed mechanism, atomic force microscopy (AFM) surface-topology images of a MAPLE glass with $T_{substrate} = 311$ K show a surface structure consisting of spherical nanoglobules (Fig. 4a). The globules range in size from ~20 to 500 nm and would each contain a few tens to thousands of polymer chains. The surface structure of the film suggests that glass formation proceeded by the assembly of polymer globules to form a nanostructured glass. Further evidence of the film morphology is obtained from cross-sectional scanning electron microscopy (SEM) images of the glasses (Fig. 4b). Clearly, sub surface nanoglobules are present. The cross-sectional images also reveal that the sub surface nanoglobules are deformed. In fact, at the polymer/substrate interface it seems that a thin polymer layer of coalesced globules has developed, which should promote structural integrity of the film.

We have explored the connection between globule and film stability by probing the temperature-dependent surface melting, that is, the coalescence of nanoglobules. Figure 4c shows that surface melting of nanoglobules does not occur until temperatures above $T_{g,standard}$. Although $T_{g,standard} = 359$ K and $T_{g,MAPLE} = 392$ K, remnants of surface nanoglobules are still present at 398 K. Hence, the surface nanoglobules are stable at elevated temperature. Figure 4d compares the temperature dependence of the WAXS peak position and the surface roughness of a film, which is an indication of nanoglobule coalescence. Remarkably, the temperature dependences of the two variables are very similar, suggesting a strong correlation between film morphology and nanoglobule stability. Furthermore, non-structured standard polymer films formed using MAPLE do not exhibit an enhanced T_g or an increase in stability.

Thus, we conclude that the global film properties are a direct manifestation of the properties of the nanoscale building blocks that constitute the film.

Our proposed mechanism of film formation is also consistent with the dependence of the thermal stability of MAPLE-deposited films on substrate temperature (Fig. 3a–c). The effect of the substrate temperature should be twofold: it should dictate the propensity of the globules to pack and the rate of glassy-state structural relaxation. In the present work, $T_{substrate} < T_{g,standard}$; thus, we classify the substrate as cold, as limited chain mobility below T_g would impede globule packing. However, the exact value of the sub-T_g substrate temperature is still important owing to the strong temperature dependence of glassy-state structural relaxation[22,37], a spontaneous relaxation process that leads to densification[38,39]. Indeed, for MAPLE-deposited PMMA films, the dependence of T_f and the rate of structural relaxation on substrate temperature seem correlated. That is, the ageing and deposition temperatures at which PMMA exhibits the maximum ageing rates and lowest values of T_f, respectively, are in a similar range. The black line in Fig. 3c represents the temperature dependence of structural relaxation for PMMA (ref. 37).

In summary, we have developed nanostructured glassy polymer films of PMMA that exhibit enhanced thermal and kinetic stability relative to the standard glass. We postulate that the ability to form stable glasses, with respect to different polymers and molecular weights, will be a general phenomenon. In practice, the properties of MAPLE-deposited glasses may make them attractive in technologies where weight and stability are central design issues. Scientifically, as they are constructed from the assembly of nearly spherical nanosized polymeric globules, MAPLE-deposited glasses represent a sort of merger between polymer and colloidal glasses, the study of which may lead to new insight about the glassy state.

Methods

Materials. Poly(methyl methacrylate) (PMMA; $M_w \sim 15,000$) and chloroform (containing amylenes as a stabilizer, ≥99%) were purchased from Sigma-Aldrich and used as received. The tacticity of PMMA was determined by NMR. A triad ratio *mm* (isotactic): *mr* (atactic): *rr* (syndiotactic) of 12.38:32.38:55.24 was calculated using the relative intensity of the peaks corresponding to the methyl groups of the MMA units.

Matrix-assisted pulsed laser evaporation (MAPLE). PMMA films were deposited on multiple substrates (silicon substrates for WAXS, XRR and FTIR, and silica for other characterization purposes, see text in the following subsections). During MAPLE deposition, a pulsed laser beam from an ArF excimer laser (Lambda Physik COMPEX205, wavelength = 193 nm, pulse duration = 20 ns) was oriented at an angle of 45° onto a frozen target rotating at 7 r.p.m. in a vacuum chamber. The MAPLE target was prepared by dissolving 0.5 wt% PMMA in chloroform. Subsequently, 10 ml of the polymer solution was poured into an aluminium cup and rapidly frozen using a liquid nitrogen bath. A cooling system was used to keep the target temperature at about 180 K during the deposition. In the MAPLE experiment, the chamber was first pumped down to a background pressure of 10^{-5} torr. During deposition, the pressure was about $2-3 \times 10^{-4}$ torr. PMMA films were deposited on a desired substrate using a pulse rate of 10 Hz and a laser fluence of 0.08 J cm^{-2}. The duration of the deposition was 1–2 h. The substrate was mounted on a heatable stage, kept a distance of 6 cm from the target, and the substrate temperature was held within ±0.5 K of the specified temperature, ranging from 300 K to 329 K. The growth rate of films in the current study was ~0.25 nm s^{-1}; as such, film formation occurs over a long time period. Therefore, ample time was available to reach a steady-state temperature based on the thermal conductivity of the film and the radiative cooling. Within experimental error, the substrate temperature and film surface temperature are the same after sufficient equilibration time. The thickness of the deposited film was measured by means of a surface profilometer (Veeco Dektak IIa).

Thermal analysis. Measurements were performed on a differential scanning calorimeter (TA Instruments Q2000). The MAPLE-deposited material on glass slides was collected carefully using a razor blade and subsequently transferred into a differential scanning calorimeter pan. The glass transition temperature of MAPLE-deposited PMMA was determined from the heating process with a temperature ramp rate of 20 K min^{-1}. We note that the glass transition temperature should be determined on cooling, but such a protocol is not possible with stable polymer glasses. For the isothermal glass-to-liquid kinetic study, temperature-modulated DSC was used. The reversing heat capacity ($C_{p,rev}$) as a function of annealing time was measured at the glass transition temperature with a modulation rate of ±0.5 K/60 s. All DSC characterizations for MAPLE-deposited PMMA, standard PMMA and hyperquenched PMMA were performed on bulk samples.

Wide-angle X-ray scattering (WAXS). WAXS scans were carried out using a Bruker D8 Discover diffractometer with a CuK$_\alpha$ radiation source (wavelength $\lambda = 0.154$ nm). The supply voltage and current were set to 40 kV and 40 mA, respectively. Samples prepared using MAPLE were deposited onto Si (5 1 0) wafers (Gem Dugout, 25 mm by 25 mm, 1 mm thick, polished one side). This crystal orientation of Si wafer was chosen owing to limited scattering within the angle range used in this study. A long Soller slit (0.12°) and a 0.6-mm-wide receiver slit were used during the experiment. Samples were scanned from 3° to 36° with a step size of 0.1° at a scan speed of 3 s per step. To determine the value of T_g, the WAXS tests were performed from room temperature to 450 K with varying temperature increments. The raw data were smoothed and plotted together for comparison; no further corrections were applied to the data. WAXS testing was also performed on a spin-coated 600-nm-thick PMMA film (of thickness comparable to the films from MAPLE) as a function of temperature. The experimental settings were the same as described above. The film was spun-cast from a toluene solution (5.0 wt% PMMA) onto a Si (5 1 0) wafer at a speed of 800 r.p.m. for 1 min. The film was dried under vacuum at $T_{g,standard}$ (359 K) for 12 h before the WAXS experiments.

Brillouin light scattering (BLS). We have employed a particular transmission scattering geometry[18] for which the phonon wave vector **q** is parallel to the film plane and its magnitude $q = (4\pi/\lambda)\sin(\theta/2)$ is independent of the refractive index and the longitudinal sound velocity $c_L = 2\pi f/q$, where $\lambda = 532$ nm is the laser wavelength in vacuum and $\theta(=90°)$ is the scattering angle. A high-resolution six-path tandem Fabry–Perot interferometer and a light-scattering set-up allowing for both q and temperature variations were used to record the BLS spectra at hypersonic frequencies. The polarization of both the incident laser beam and the scattered light was selected to be perpendicular to the scattering (sagittal) plane to measure the polarized BLS spectra and obtain c_L. Temperature-dependent BLS spectra were recorded by placing the substrate-supported glass films into a heating chamber, and the samples were heated from room temperature to 423 K in multiple steps. For each measurement the sample was stabilized for about 15 min before recording the BLS spectrum, which was acquired over about 20 min.

Owing to the turbidity of the MAPLE-deposited glasses, BLS spectra could be recorded at temperatures only above ~360 K. On the other hand, access to the BLS spectra of the MAPLE-deposited glasses at ambient temperatures was enabled by quenching these films from $T \sim T_{g,standard}$ to room temperature (see, for example, the lower inset of Fig. 2c).

References

1. Angell, C. A. Formation of glasses from liquids and biopolymers. *Science* **267**, 1924–1935 (1995).
2. Debenedetti, P. G. & Stillinger, F. H. Supercooled liquids and the glass transition. *Nature* **410**, 259–267 (2001).
3. Ediger, M. D., Angell, C. A. & Nagel, S. R. Supercooled liquids and glasses. *J. Phys. Chem.* **100**, 13200–13212 (1996).
4. McKenna, G. B. *Glass Formation and Glassy Behavior* (Pergamon, 1989).
5. Badrinarayanan, P., Zheng, W., Li, Q. & Simon, S. L. The glass transition temperature versus the fictive temperature. *J. Non-Cryst. Solids* **353**, 2603–2612 (2007).
6. Swallen, S. F. *et al.* Organic glasses with expectional thermodynamic and kinetic stability. *Science* **315**, 353–356 (2007).
7. Kearns, K. L., Still, T., Fytas, G. & Ediger, M. D. High-modulus organic glasses prepared by physical vapor deposition. *Adv. Mater.* **22**, 39–42 (2010).
8. Kearns, K. L., Swallen, S. F., Ediger, M. D., Wu, T. & Yu, L. Influence of substrate temperature on the stability of glasses prepared by vapor deposition. *J. Chem. Phys.* **127**, 154702 (2007).
9. Kearns, K. L., Swallen, S. F., Ediger, M. D., Wu, T. & Yu, L. Hiking down the energy landscape: Progress toward the Kauzmann temperature via vapor deposition. *J. Phys. Chem. B* **112**, 4934–4942 (2008).
10. Swallen, S. F., Traynor, K., McMahon, R. J., Ediger, M. D. & Mates, T. E. Stable glass transformation to supercooled liquid via surface-initiated growth front. *Phys. Rev. Lett.* **102**, 065503 (2009).
11. Leon-Gutierrez, E., Garcia, G., Lopeandia, A. F., Clavaguera-Mora, M. T. & Rodriquez-Viejo, J. Size effects and extraordinary stability of ultrathin vapor deposited glassy films of toluene. *J. Phys. Chem. Lett.* **1**, 341–345 (2010).
12. Ishii, K., Nakayama, H., Hirabayashi, S. & Moriyama, R. Anomalously high-density glass of ehtylbenzene prepared by vapour deposition at temperatures close to the glass-transition temperature. *Chem. Phys. Lett.* **459**, 109–112 (2008).
13. Pique, A. *et al.* Growth of organic thin films by the matrix assisted pulsed laser evaporation (MAPLE) technique. *Thin Solid Films* **355**, 536–541 (1999).
14. Chrisey, D. B. *et al.* Laser deposition of polymer and biomaterial films. *Chem. Rev.* **103**, 553–576 (2003).
15. Angell, C. A. & Wang, L-M. Hyperquenching and cold equilibration strategies for the study of liquid–liquid and protein folding transitions. *Biophys. Chem.* **105**, 621–637 (2003).
16. Johari, G. P. Calorimetric features of high enthalpy amorphous solids and glass softening temperature of water. *J. Phys. Chem. B* **107**, 9063–9070 (2003).
17. Stillinger, F. H. A topographic view of supercooled liquids and glass formation. *Science* **267**, 1935–1939 (1995).
18. Cheng, W. *et al.* Elastic properties and glass transition of supported polymer thin films. *Macromolecules* **40**, 7283–7290 (2007).
19. Dawson, K. J., Kearns, K. L., Yu, L., Steffen, W. & Ediger, M. D. Physical vapor deposition as a route to hidden amorphous states. *Proc. Natl Acad. Sci. USA* **106**, 15165–15170 (2009).
20. Fakhraai, Z. & Forrest, J. A. Measuring the surface dynamics of glassy polymers. *Science* **319**, 600–604 (2008).
21. Ellison, C. J. & Torkelson, J. M. The distribution of glass transition temperatures in nanoscopically confined glass formers. *Nature Mater.* **2**, 695–700 (2003).
22. Priestley, R. D., Ellison, C. J., Broadbelt, L. J. & Torkelson, J. M. Structural relaxation of polymer glasses at surfaces, interfaces, and in between. *Science* **309**, 456–459 (2005).
23. Peter, S., Meyer, H. & Baschnagel, J. Thickness-dependent reduction of the glass-transition temperature in thin polymer films with a free surface. *J. Polym. Sci. B* **44**, 2951–2967 (2006).
24. Torres, J. A., Nealey, P. F. & de Pablo, J. J. Molecular simulation of ultrathin polymeric films near the glass transition. *Phys. Rev. Lett.* **85**, 3221–3224 (2000).
25. Shi, Z., Debenedetti, P. G. & Stillinger, F. H. Properties of model atomic free-standing thin films. *J. Chem. Phys.* **134**, 114524 (2011).
26. Singh, S. & de Pablo, J. J. A molecular view of vapor deposited glasses. *J. Chem. Phys.* **134**, 194903 (2011).
27. Sellinger, A., Leveugle, E., Fitz-Gerald, J. M. & Zhigilei, L. V. Generation of surface features in films deposited by matrix assisted pulsed laser evaporation: The effects of the stress confinement and droplet landing velocity. *Appl. Phys. A* **92**, 821–829 (2008).
28. Sima, F. *et al.* Levan nanostructured thin films by MAPLE assembling. *Biomacromolecules* **12**, 2251–2256 (2011).

29. Leveugle, E. & Zhigilei, L. V. Molecular dynamics simulation study of the ejection and transport of polymer molecules in matrix-assisted pulsed laser evaporation. *J. Appl. Phys.* **102,** 074914 (2007).
30. Zhigilei, L. V., Volkov, A. N., Leveugle, E. & Tabetah, M. The effect of the target structure and composition on the ejection and transport of polymer molecules and carbon nanotubes in matrix-assisted pulsed laser evaporation. *Appl. Phys. A* **105,** 529–546 (2011).
31. De Gennes, P. G. Kinetics of collapse for a flexible coil. *J. Phys. Lett.* **46,** 639–642 (1985).
32. Aseyev, V., Tenhu, H. & Winnik, F. M. Temperature dependence of the colloidal stability of neutral amphiphilic polymers in water. *Adv. Polym. Sci.* **196,** 1–85 (2006).
33. McKenna, G. B. Glassy states: Concentration glasses and temperature glasses compared. *J. Non-Cryst. Solids* **353,** 3820–3828 (2007).
34. Zheng, Y., Priestley, R. D. & McKenna, G. B. Physical aging of an epoxy subsequent to relative humidity jumps through the glass concentration. *J. Polym. Sci. B* **42,** 2107–2121 (2004).
35. Mi, Y., Xue, G. & Lu, X. A new perspective of the glass transition of polymer single-chain nanoglobules. *Macromolecules* **36,** 7560–7566 (2003).
36. Mi, Y., Xue, G. & Wang, X. Glass transition of nano-sized single chain globules. *Polymer* **43,** 6701–6705 (2002).
37. Greiner, R. & Schwarzl, F. R. Thermal contraction and volume relaxation of amorphous polymers. *Rheol. Acta* **23,** 378–395 (1984).
38. Hodge, I. A. Physical aging in polymer glasses. *Science* **267,** 1945–1947 (1995).
39. Hutchinson, J. M. Physical aging of polymers. *Prog. Polym. Sci.* **20,** 703–760 (1995).

Author contributions

Y.G. designed and set up the MAPLE system, performed experiments on MAPLE, DSC, GPC, NMR, WAXS, XRR, refractive index, temperature-dependent AFM, discussed and analysed the results and wrote the manuscript. A.M. designed the MAPLE system, and carried out laser calibration and trouble-shooting. D.S. performed BLS and SEM measurements. J.W.C. performed NMR and WAXS measurements and discussed the results. C.Z. performed MAPLE experiments. M.W. performed FTIR and AFM measurements. N.Y. assisted in WAXS and XRR characterization and provided equipment for temperature control on AFM. G.F. coordinated the BLS study, discussed results and commented on the manuscript. C.B.A. coordinated the set up of the MAPLE system, discussed the results and commented on the manuscript. R.D.P. conceived the idea, coordinated the project, discussed the results and wrote the manuscript.

Additional information

The authors declare no competing financial interests. Supplementary information accompanies this paper on www.nature.com/naturematerials. Reprints and permissions information is available online at www.nature.com/reprints. Correspondence and requests for materials should be addressed to R.D.P.